

Electronic Supplementary Information

Trimorphism of *N*-(3-Pyridyl)-Benzamide

Christian Näther, Inke Jess, Julia Bahrenburg, Dennis Bank and Friedrich Temps

Content

Fig. S1	Microscopic image of the crystals obtained by recrystallization of the compound from ethylacetate and of the same batch after two days.	2
Fig. S2	Experimental X-ray powder pattern of a batch that was stored for two days at room-temperature and calculated pattern for form I .	3
Tab. S1	Melting temperatures as well as melting enthalpy for form I , obtained from several DSC runs at different heating rates.	3
Fig. S3	Experimental X-ray powder pattern of the solidified melt obtained from an DSC measurement and calculated pattern for form I .	4
Fig. S4	DSC measurements of form I measured at different heating rates.	4
Fig. S5	DSC measurement of form I at 20°C/min.	5
Fig. S6	Experimental X-ray powder pattern of the residue obtained by fast crystallization and of that obtained after the first endothermic event if this mixture is heated in a DCS measurement and calculated powder pattern for form II and form I .	5
Fig. S7	DSC curves of a mixture of form I and form II measured at different heating rates.	6
Fig. S8	Experimental X-ray powder pattern of the residue obtained after storing a mixture of form I and form II in a refrigerator at -20°C and calculated powder pattern for form I .	7
Fig. S9	Experimental X-ray powder pattern of the residues obtained after stirring form I in different solvents and calculated powder pattern for form I .	7
Fig. S9	Experimental X-ray powder pattern of the residues obtained after stirring form I in different solvents and calculated powder pattern for form I .	8
Fig. S10	Figure S10. Experimental X-ray powder pattern of the residue obtained after sublimation and spontaneous crystallization and calculated powder pattern for form I .	8
Fig. S11	Experimental X-ray powder pattern of the residue obtained by mixing a saturated solution of the compound with n-hexane and calculated powder pattern for form I .	8
Fig. S12	Selected microscopic images of form I at selected temperatures obtained at 3°C/min.	9
Fig. S13	Selected microscopic images of form II at selected temperatures obtained at 3°C/min.	10
Fig. S14	Selected microscopic images of form III at different temperatures obtained at 3°C/min.	11
Fig. S15	Selected microscopic images of form I , II and III at different temperatures obtained at 3°C/min, showing the polymorphic transitions of form II and III .	12
Fig. S16	Selected microscopic images of form I , II and III at different temperatures obtained at 3°C/min, showing the polymorphic transitions of form II and III , showing the melting of these forms.	13

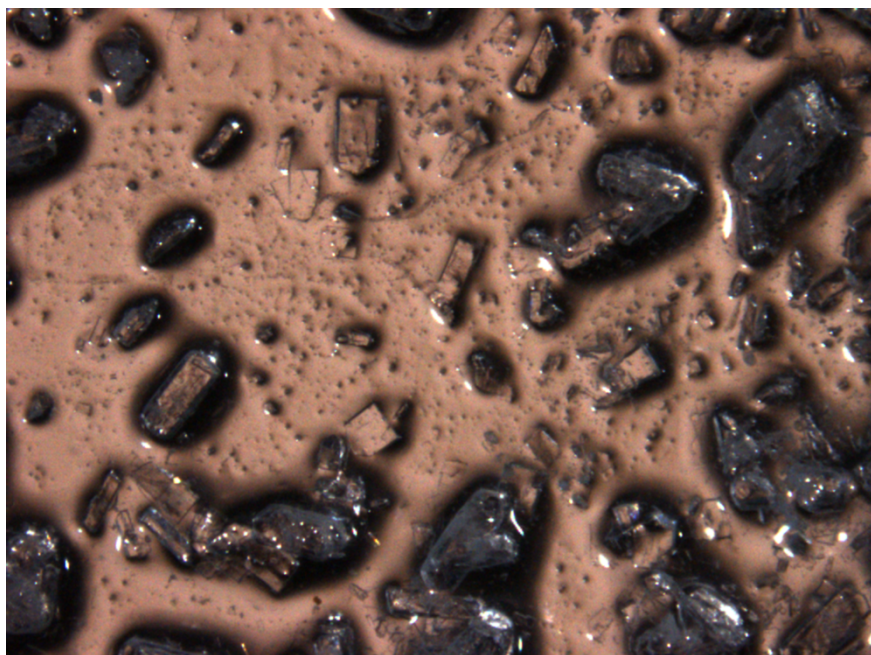


Figure S1. Microscopic image of the crystals obtained by recrystallization of the compound from ethylacetate (top) and of the same batch after two days. The batch shown above consists of form **II** and **III**, whereas the batch shown below consists of form **I** exclusively (see Figure S2).

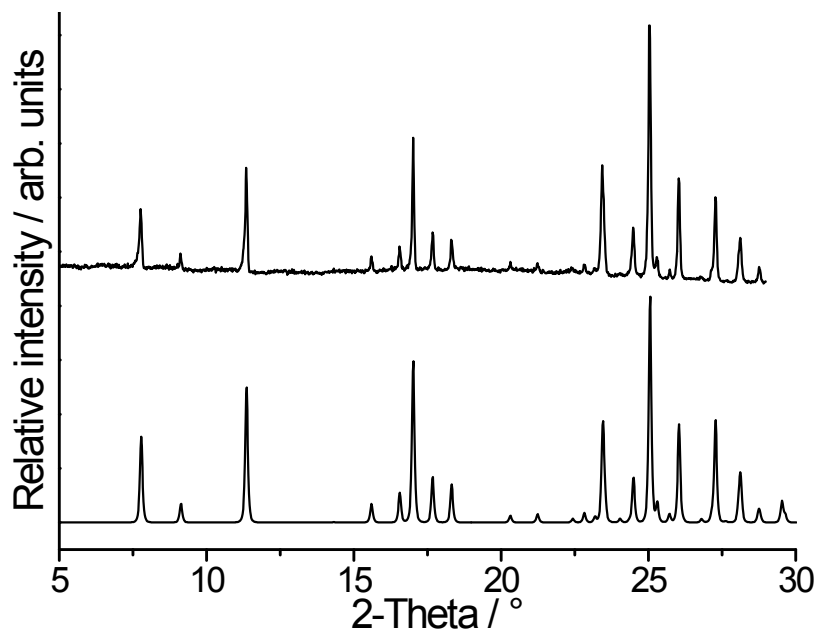


Figure S2. Experimental X-ray powder pattern of a batch that was stored for two days at room-temperature (top) and calculated pattern for form **I**. Please note that this batch consists in the beginning of form **II** and **III**, which is also obvious from figure S1: top).

Table S1: Melting temperatures as well as melting enthalpy for form **I**, obtained from several DSC runs at different heating rates.

	Heating rate/ °C/min	$\Delta H_{\text{fus}} /$ KJ/mol	Onset temperature in °C	Peak temperature in °C
1st heating	1	22.6	115.6	116.5
2nd heating	1	22.6	115.7	116.3
3rd heating	1	22.5	115.6	116.5
1st heating	3	22.7	115.7	116.8
2nd heating	3	22.9	115.6	116.7
3rd heating	3	22.9	115.6	116.7
1st heating	5	21.9	115.5	116.8
2nd heating	5	21.9	115.4	116.9
3rd heating	5	22.0	115.3	116.9
1st heating	10	22.0	115.4	117.5
2nd heating	10	21.9	115.2	117.5
3rd heating	10	21.8	115.2	117.4
1st heating	20	23.7	115.8	118.1
2nd heating	20	23.4	115.7	118.0
3rd heating	20	23.4	115.7	118.2
Average	-	22.5	115.5	-

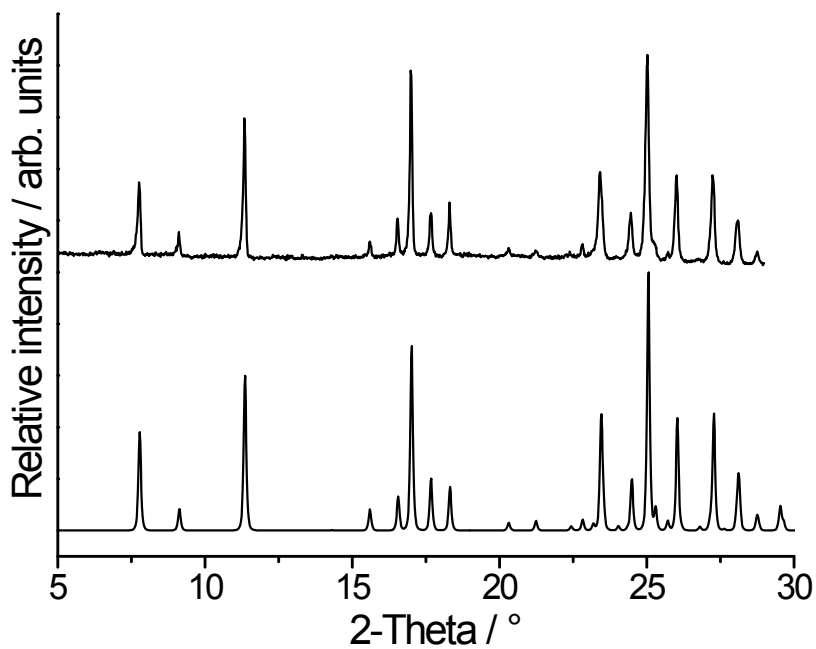


Figure S3. Experimental X-ray powder pattern of the solidified melt obtained from an DSC measurement (top) and calculated pattern for form **I**.

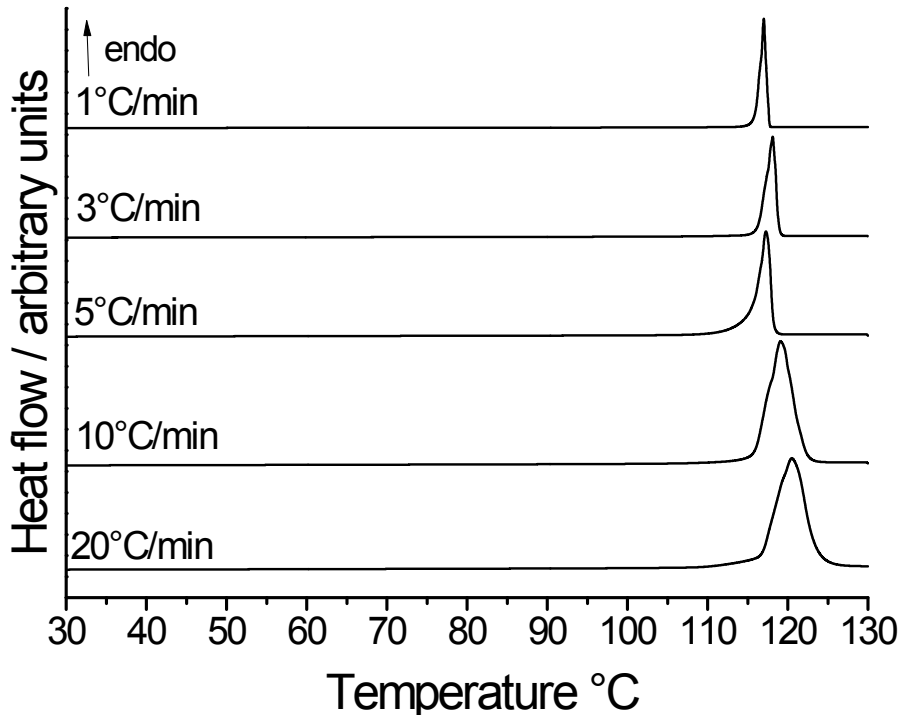


Figure S4. DSC curves of form **I** measured at different heating rates.

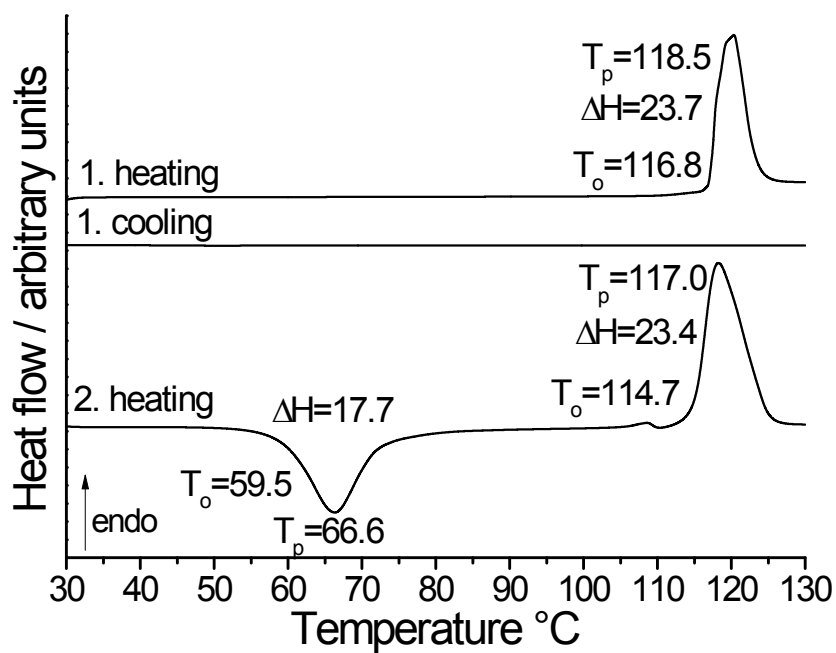


Figure S5. DSC curves of form **I** at 20°C/min. Given is the melting and crystallization enthalpy in kJ/mol and the peak (T_p) and onset (T_o) temperatures in °C.

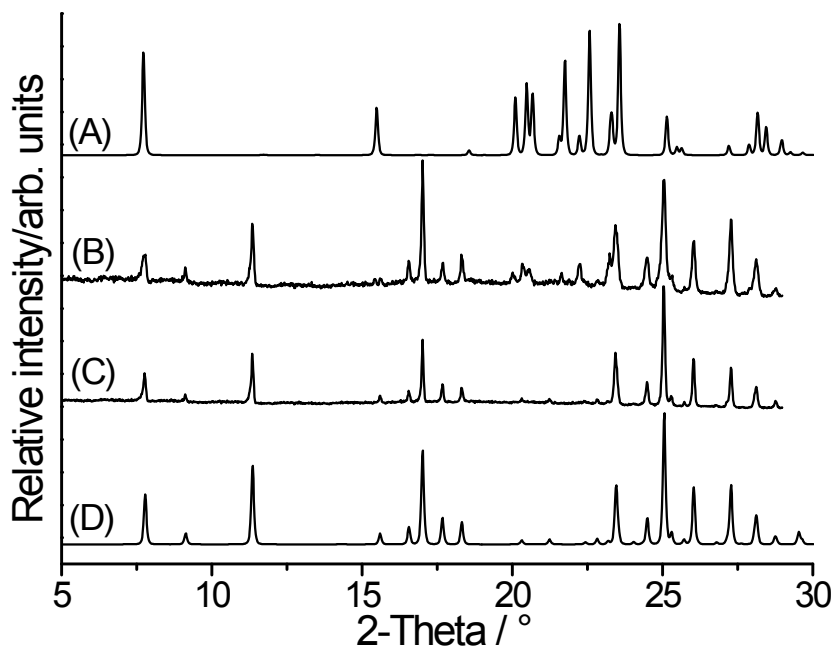


Figure S6. Experimental X-ray powder pattern of the residue obtained by fast crystallization (B) and of that obtained after the first endothermic event if this mixture is heated in a DCS measurement (C) and calculated powder pattern for form **II** (A) and form **I** (D).

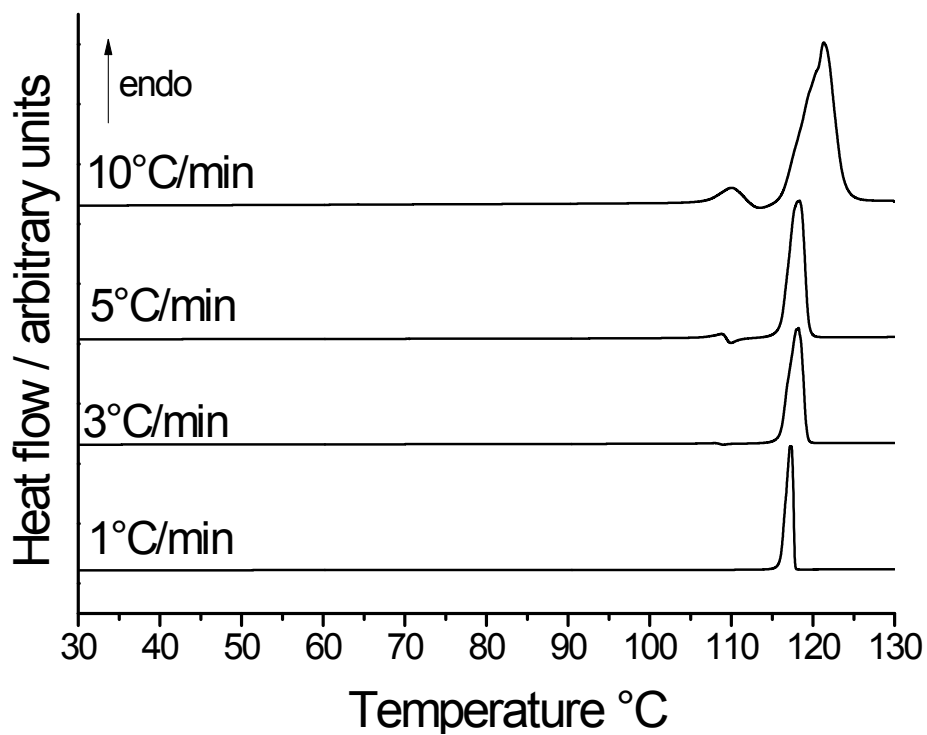
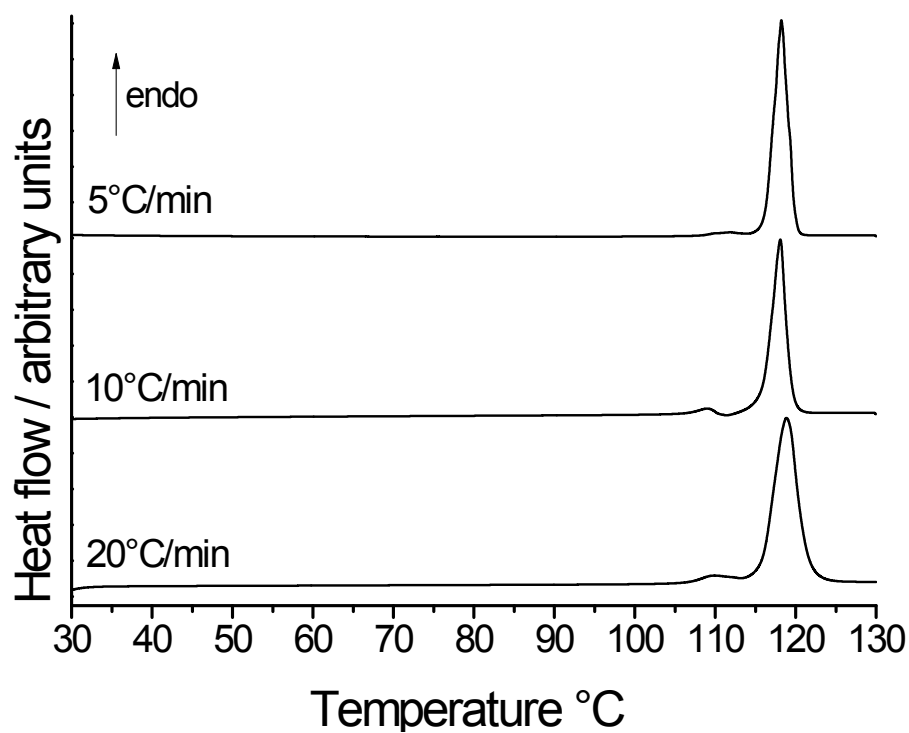


Figure S7. DSC curves for two different batches of a mixture of form I and form II measured at different heating rates.

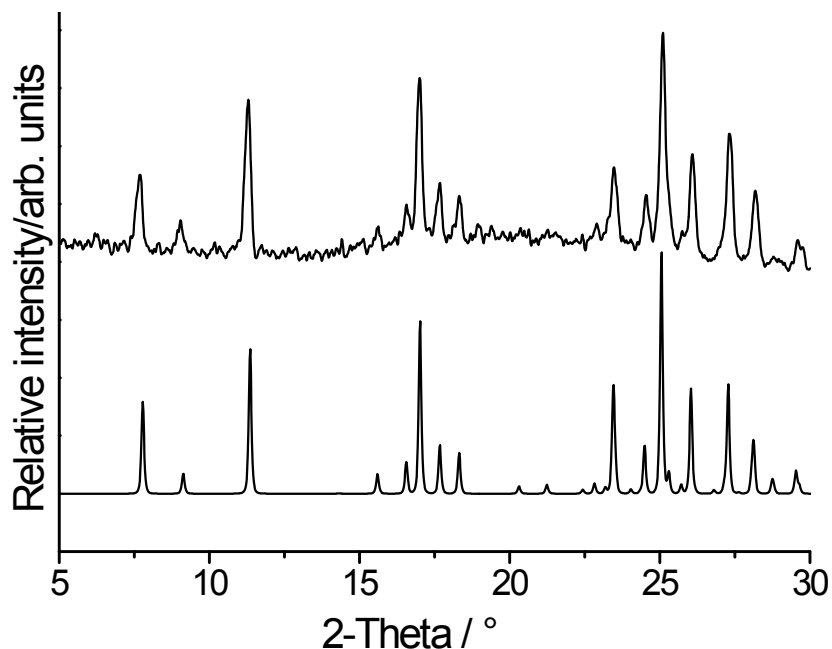


Figure S8. Experimental X-ray powder pattern of the residue obtained after storing a mixture of form **I** and form **II** in a refrigerator at -20°C (top) and calculated powder pattern for form **I** (bottom).

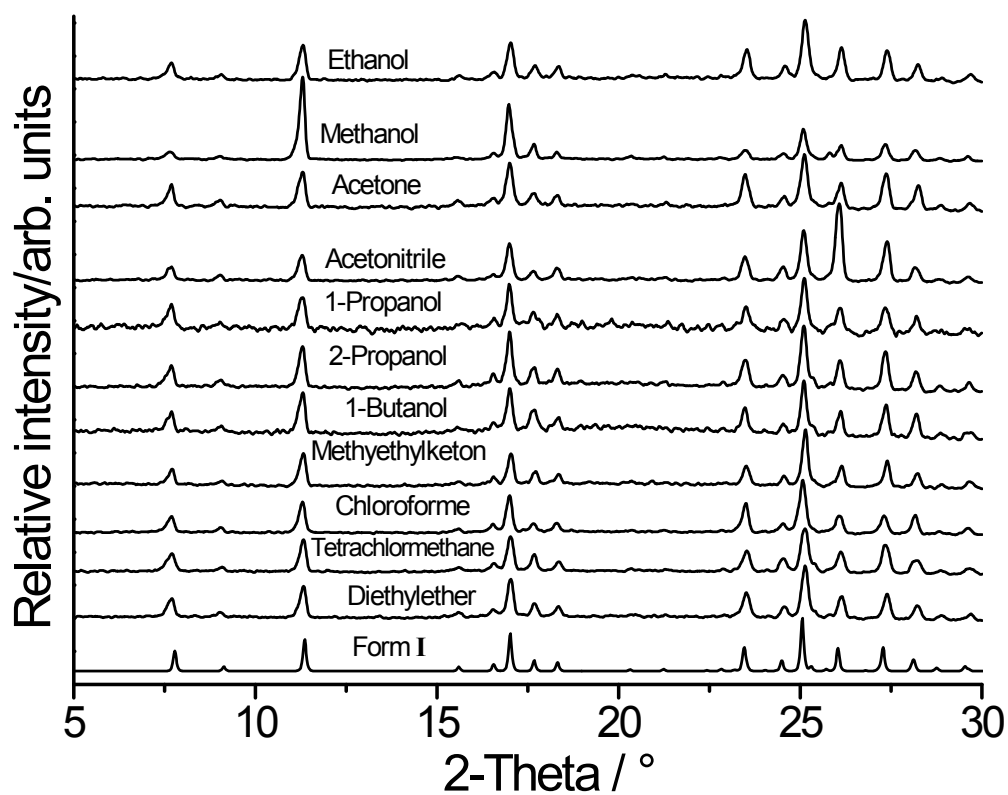


Figure S9. Experimental X-ray powder pattern of the residues obtained after stirring form **I** in different solvents and calculated powder pattern for form **I**.

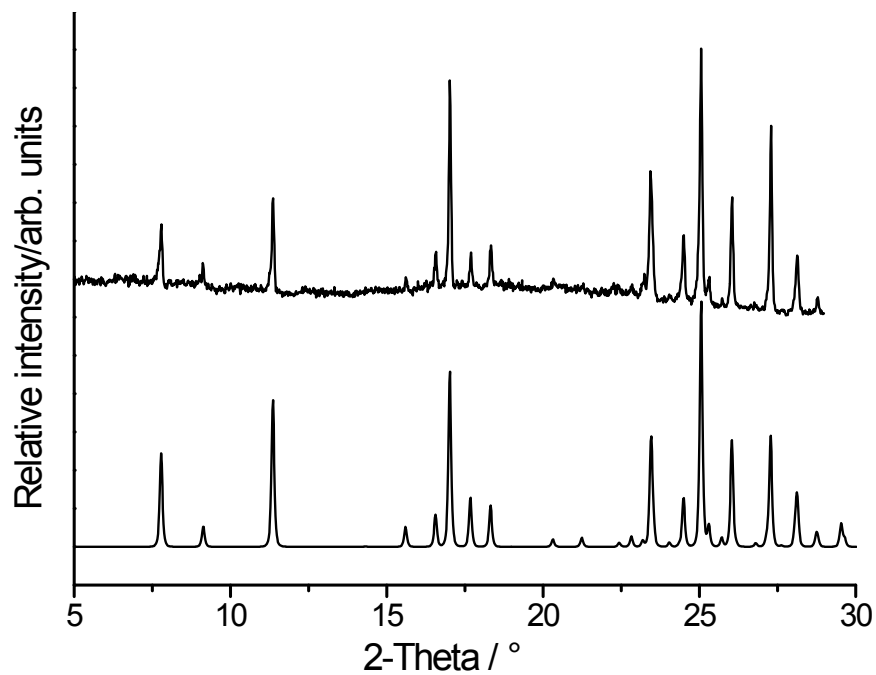


Figure S10. Experimental X-ray powder pattern of the residue obtained after sublimation and spontaneous crystallization (top) and calculated powder pattern for form **I** (bottom).

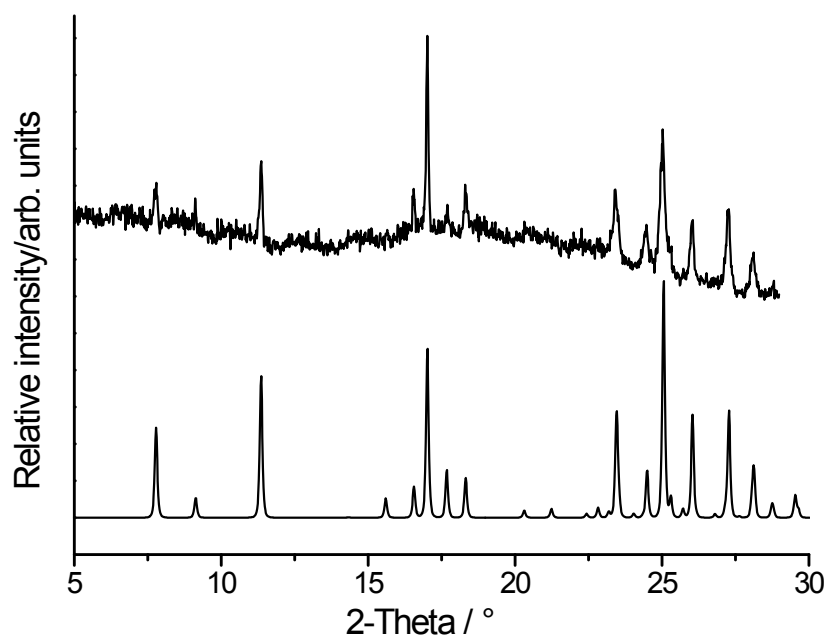


Figure S11. Experimental X-ray powder pattern of the residue obtained by mixing a saturated solution of the compound with n-hexane (top) and calculated powder pattern for form **I** (bottom).

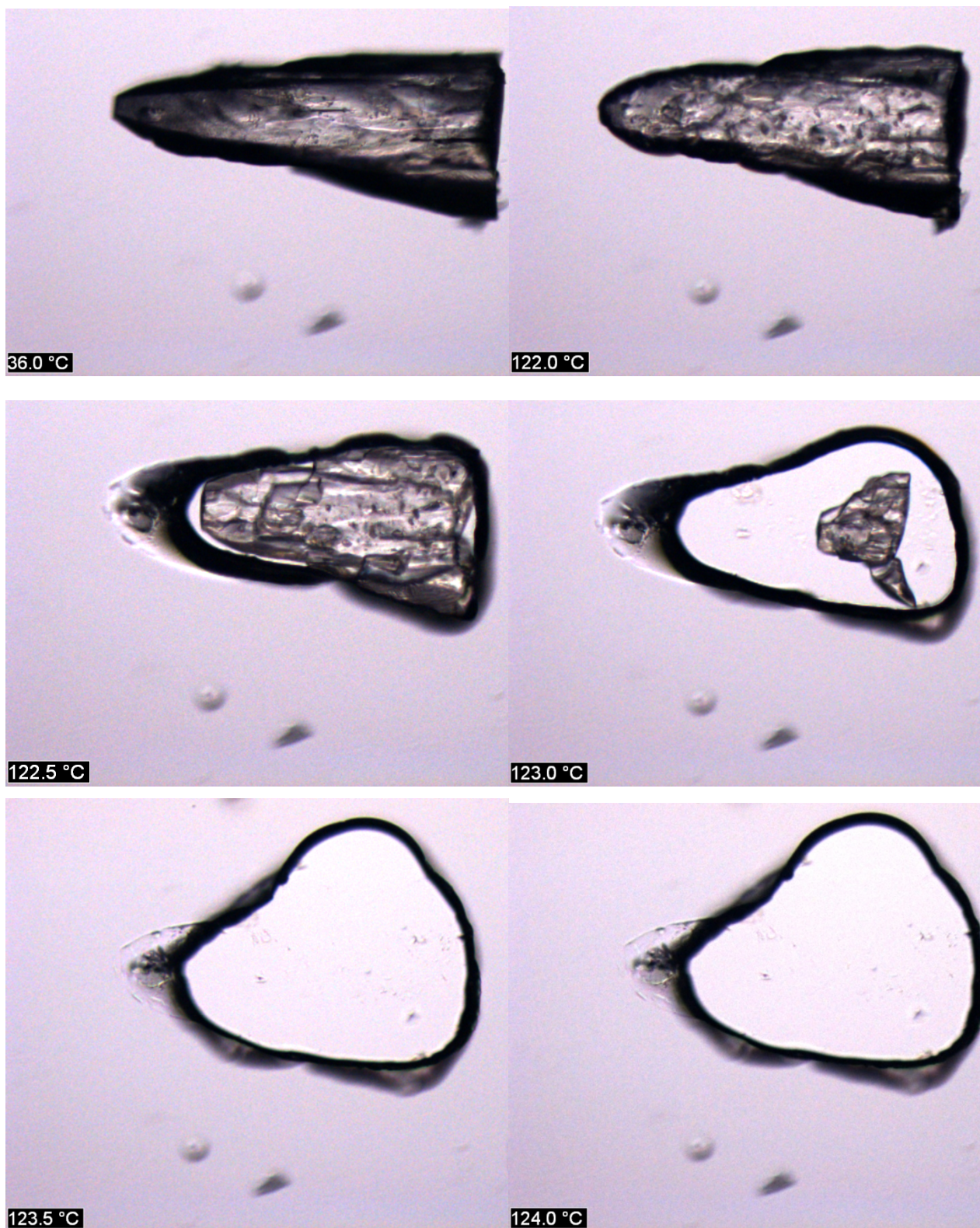


Figure S12. Selected microscopic images of form **I** at selected temperatures obtained at 3°C/min. In this case melting is observed at about 122.5°C.

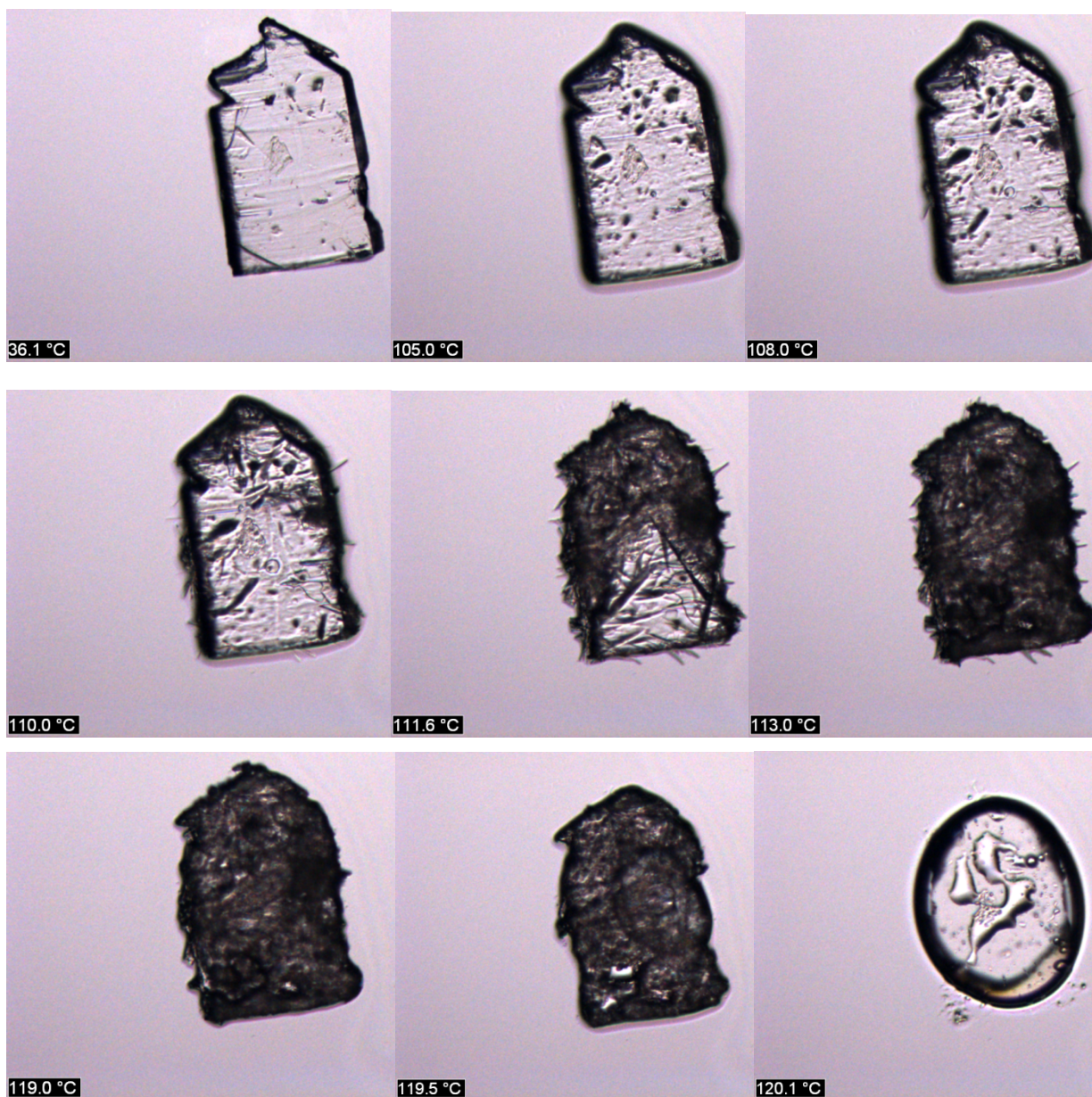


Figure S13. Selected microscopic images of form **II** at selected temperatures obtained at 3°C/min. The polymorphic transition is observed starting at about 105°C and melting is observed at about 120°C.

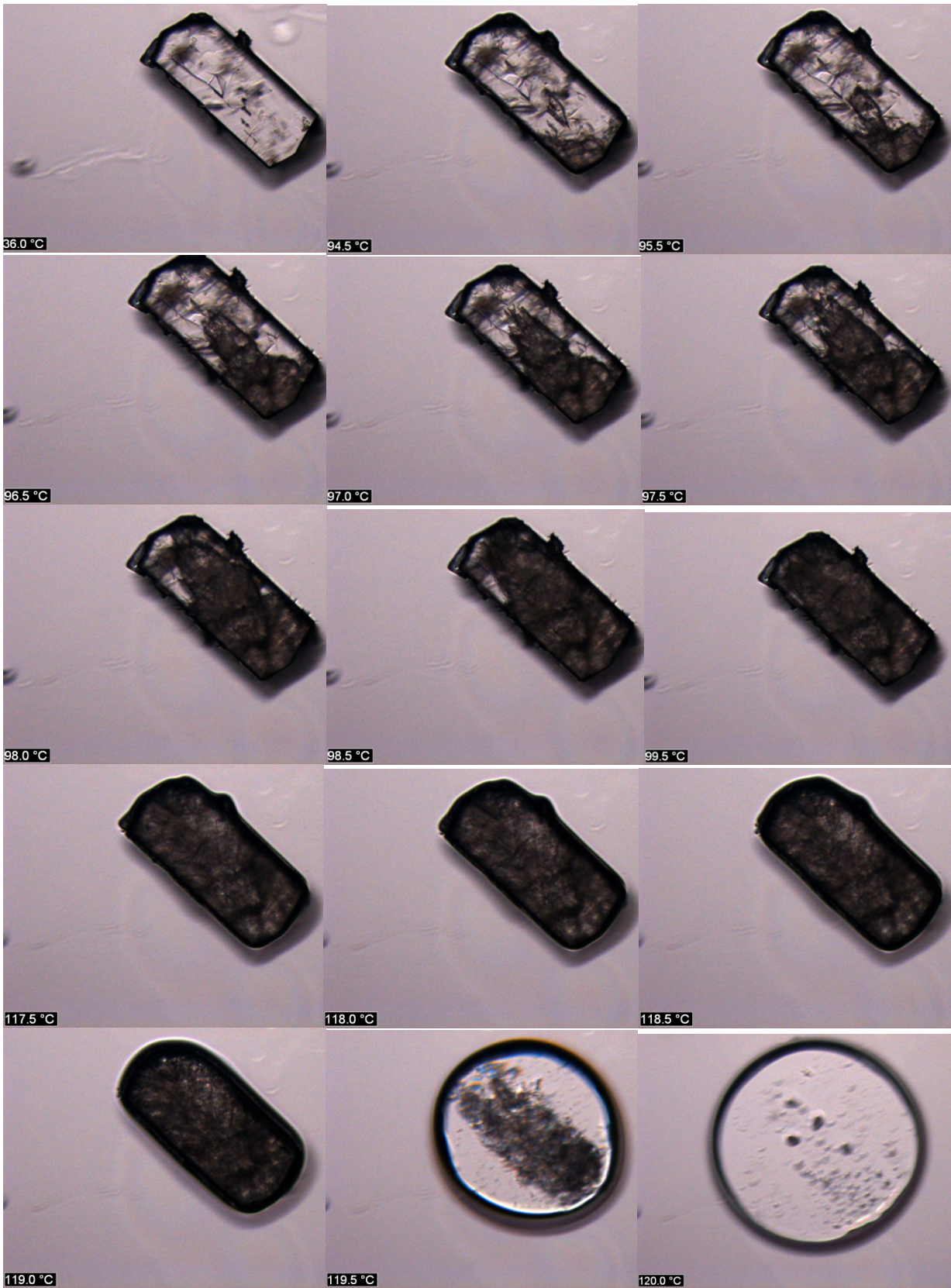


Figure S14. Selected microscopic images of form **III** at different temperatures obtained at 3°C/min, showing the polymorphic transition starting at about 96°C and the melting at about 119°C.

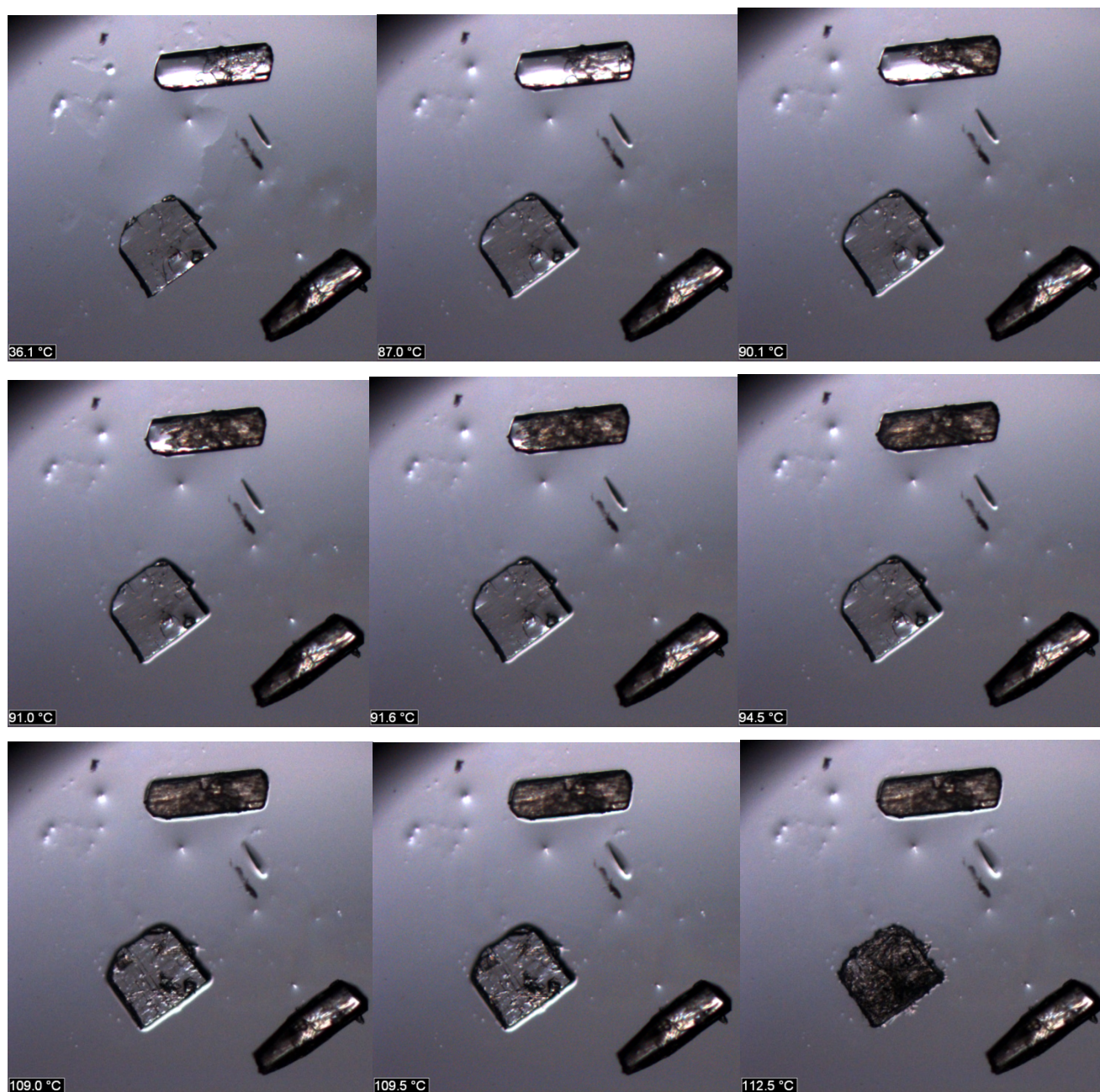


Figure S15. Selected microscopic images of form **I** (bottom: right), **II** (bottom: left) and **III** (top) at different temperatures obtained at 3°C/min, showing the polymorphic transitions of form **II** and **III**.

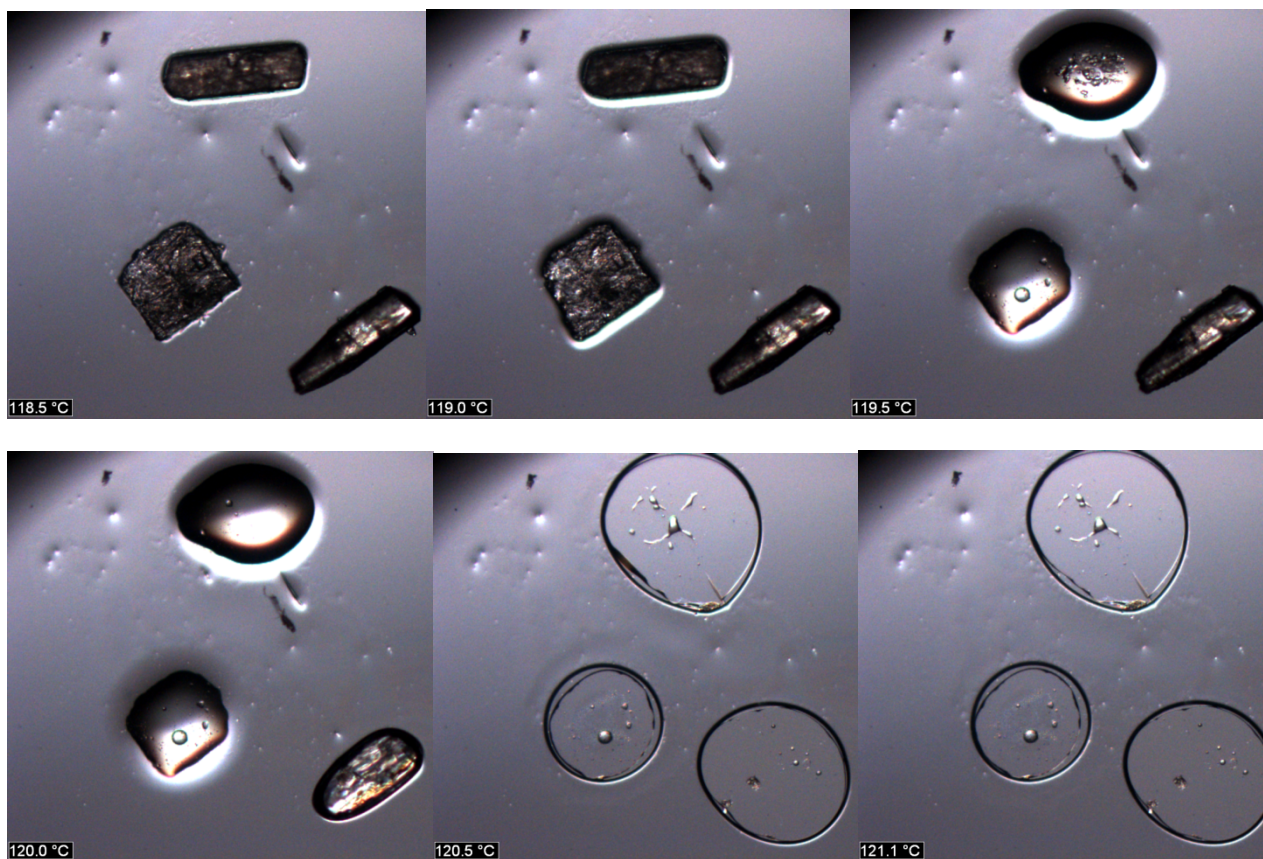


Figure S16. Selected microscopic images of form **I** (bottom: right), **II** (bottom: left) and **III** (top) at different temperatures obtained at 3°C/min, showing the melting of these forms.